

Improved measurement of carbonaceous aerosol: evaluation of the sampling artifacts and inter-comparison of the thermal-optical analysis methods

Y. Cheng¹, K. B. He¹, F. K. Duan¹, M. Zheng², Y. L. Ma¹, J. H. Tan¹, and Z. Y. Du¹

¹State Key Joint Laboratory of Environment Simulation and Pollution Control, Department of Environmental Science and Engineering, Tsinghua University, Beijing, China

²School of Earth and Atmospheric Sciences, Georgia Institute of Technology, Atlanta, Georgia, USA

Received: 8 June 2010 – Published in Atmos. Chem. Phys. Discuss.: 25 June 2010

Revised: 23 August 2010 – Accepted: 8 September 2010 – Published: 10 September 2010

Abstract. The sampling artifacts (both positive and negative) and the influence of thermal-optical methods (both charring correction method and the peak inert mode temperature) on the split of organic carbon (OC) and elemental carbon (EC) were evaluated in Beijing. The positive sampling artifact constituted 10% and 23% of OC concentration determined by the bare quartz filter during winter and summer, respectively. For summer samples, the adsorbed gaseous organics were found to continuously evolve off the filter during the whole inert mode when analyzed by the IMPROVE-A temperature protocol. This may be due to the oxidation of the adsorbed organics during sampling (reaction artifact) which would increase their thermal stability. The backup quartz approach was evaluated by a denuder-based method for assessing the positive artifact. The quartz-quartz (QBQ) in series method was demonstrated to be reliable, since all of the OC collected by QBQ was from originally gaseous organics. Negative artifact that could be adsorbed by quartz filter was negligible. When the activated carbon impregnated glass fiber (CIG) filter was used as the denuded backup filter, the denuder efficiency for removing gaseous organics that could be adsorbed by the CIG filter was only about 30%. EC values were found to differ by a factor of about two depending on the charring correction method. Influence of the peak inert mode temperature was evaluated based on the summer samples. The EC value was found to continuously decrease with the peak inert mode temperature. Premature evolution of light absorbing carbon began when the peak inert mode

temperature was increased from 580 to 650 °C; when further increased to 800 °C, the OC and EC split frequently occurred in the He mode, and the last OC peak was characterized by the overlapping of two separate peaks. The discrepancy between EC values defined by different temperature protocols was larger for Beijing carbonaceous aerosol compared with North America and Europe, perhaps due to the higher concentration of brown carbon in Beijing aerosol.

1 Introduction

Carbonaceous aerosol, a major component in PM_{2.5}, consists of organic carbon (OC) and elemental carbon (EC). It is important due to its complex effects on multiple geographical scales, such as human health, haze, hydrological cycle, and climate change. As a result, continuing and increasing attention has been paid to carbonaceous aerosol. However, carbonaceous aerosol is not well understood, including its source (primary and secondary), atmospheric process (physical and chemical) and impacts (on human health and environment), compared with the other components in PM_{2.5} (e.g., water-soluble inorganic ions and mineral dust). One of the difficult challenges is how to minimize the uncertainties in the measurement of carbonaceous aerosol. Factors concerned are described below.

(1) Sampling artifact. Quartz filters are typically used for the sampling and subsequently analysis of carbonaceous aerosol, mainly due to their thermal stability. The quartz filter has a large surface area upon which adsorption of gaseous organics could occur, causing the positive artifact. On the other hand, volatilization of the collected particulate organic



Correspondence to: K. B. He
(hekb@tsinghua.edu.cn)

carbon would induce the negative artifact. The positive artifact usually coexists with the negative artifact, which confuses the approaches to eliminate or minimize the artifacts. Cadle et al. (1983) found substantial OC on the backup quartz filter placed behind a front quartz filter (quartz behind quartz, QBQ). But the origin of this carbon, whether from the originally gaseous organics or from the volatilized particulate OC, was not known, which limited the attempted correction using the backup filter data. A similar configuration using Teflon and quartz filter (quartz behind Teflon, QBT) in series has been adopted since early 1990s (Hering et al., 1990). But the origin of the OC measured by the backup filter (backup OC), either QBQ or QBT, remained unclear. Results from the micro-orifice uniform deposit impactor (MOUDI) sampler (McMurry and Zhang, 1989) provided indirect evidence for the origin of backup OC, in which 70% of the OC and 17% of the EC was found to be on the quartz after-filter. Since it was unlikely that such a high fraction of OC would be associated with particles smaller than $0.10\ \mu\text{m}$, it was concluded that the after-filter OC was dominated by the adsorbed organics originally in gas phase. McDow and Huntzicker (1990) found a decrease in the OC concentration determined by the bare quartz filter with increasing face velocity, and the dependence was removed when backup OC was subtracted, providing additional indirect evidence for the origin of backup OC.

Clearly, filtration methods alone can not quantify the sampling artifacts, since the adsorption and volatilization process can not be separated. As a result, separating particulate matter from potential interfering gaseous organics before filtration is essential, giving rise to the organic denuder technology. The organic denuder is a device which removes gaseous organics by diffusion to an adsorbent surface but allows nearly all of the particulate matter to pass through. Strips of quartz filter were first used as an organic denuder (Fitz, 1990). Several other configurations were developed since then, such as the CIF denuder containing strips of CIF (activated carbon impregnated cellulose filter) filter (Eatough et al., 1993), the activated carbon filled (ACF) denuder (Viana et al., 2006a), the activated carbon monolith tube (ACM) denuder (Subramanian et al., 2004), and the annular (Gundel et al., 1995) and honeycomb (Mader et al., 2001) XAD (polystyrene – divinylbenzene resin) denuder.

One of the most substantial concerns when using organic denuder is its efficiency for removing gaseous organics that may be adsorbed by the filters downstream. Activated carbon-based denuders have been demonstrated to have a higher efficiency and a much longer useful time compared with XAD-based denuder (Lewtas et al., 2001; Cheng et al., 2009a). For example, an average efficiency of 95%, varying from 91% to 97%, was obtained over a six-month period for the CIF denuder operated at 40 L/min (Eatough et al., 1999), whereas the 8-channel, 60 cm-long XAD annular denuder could only be used for less than 20 h at a sampling rate of 16.7 L/min (Fan et al., 2003). Moreover, when operat-

ing the XAD-based denuder, it takes a significant amount of human and material resources and typically requires an on-site laboratory (Swartz et al., 2003). As a result, Cheng et al. (2009a) suggested that the activated carbon-based denuders were more suitable for the routine monitoring of OC and EC. However, this does not mean the XAD-based denuder is useless, since it has been typically used for the research of the gas-particle partitioning of PAHs in which the XAD denuder was extracted after each sampling run (Gundel et al., 1995; Lane et al., 2000; Swartz et al., 2003).

(2) Split of OC and EC. The thermal-optical method developed by Huntzicker et al. (1982) is a conventional approach for classifying carbonaceous aerosol into OC and EC. Ideally, a portion of a loaded quartz filter is exposed to a prescribed temperature protocol first in an inert atmosphere (such as 100%He) to determine OC and then in an oxidizing atmosphere (such as He/O₂) to determine EC. A major complication is that a fraction of OC chars or pyrolyzes during the inert mode of the analysis. This charring can absorb light (which results in the drop of both the filter transmittance and reflectance) and requires an oxidizing atmosphere to evolve off the filter. This fraction of OC is usually called pyrolyzed organic carbon (PC), which is quantified as the carbon evolved in the oxidizing atmosphere that is necessary to return the filter transmittance or reflectance to its initial value. The PC correction in the thermal-optical method depends on one of the following two assumptions: (i) PC evolves before the native EC in the oxidizing atmosphere, or (ii) PC and native EC have the same light attenuation coefficient (Yang and Yu, 2002). But both of these assumptions have been demonstrated to be invalid (Yang and Yu, 2002; Yu et al., 2002; Chow et al., 2004; Subramanian et al., 2006; Cheng et al., 2009b), which results in a systemic artifact for the split of OC and EC. Previous studies have shown that EC would be under-estimated by the operationally defined value (determined by the transmittance correction), since PC is co-evolved with native EC and is darker in color (Chow et al., 2004; Subramanian et al., 2006; Cheng et al., 2009b).

Despite the limitations mentioned above, the thermal-optical method is widely used, and a variety of operational protocols have been employed (Watson et al., 2005), which differ mainly with respect to (i) temperature protocol, including temperature plateau and residence time at each plateau, and (ii) charring correction by light reflectance or transmittance. Chow et al. (2004) has demonstrated that substantial charring takes place within the filter; the drop of filter transmittance in the inert mode is influenced by the char formed throughout the filter thickness, whereas the drop of reflectance is dominated by charring of the near-surface organics. As a result, EC values defined by transmittance correction were usually lower than that defined by reflectance correction (Chow et al., 2001, 2004, 2009).

Importantly, measured EC values have been shown to vary significantly among the various temperature protocols (Schauer et al., 2003a; Subramanian et al., 2006), and the

discrepancies depend on the aerosol composition, both organic and inorganic (Yu et al., 2002). The temperature of the last step in the inert mode, which is usually called the peak inert mode temperature, has been demonstrated to be the key factor that influences the split of OC and EC defined by different protocols (Conny et al., 2003; Schauer et al., 2003a; Subramanian et al., 2006). Two kinds of artifacts can be attributed to the influence of the peak inert mode temperature: too high a peak inert mode temperature may underestimate the EC concentration due to the premature evolution of light absorbing carbon (including both PC and native EC), while too low a peak inert mode temperature may overestimate the EC concentration due to the incomplete evolution of OC. Both artifacts may be detected by tracking the filter transmittance signal which can reflect the process of PC formation and the evolution of light absorbing carbon (including both PC and native EC) throughout the filter thickness. Premature evolution of light absorbing carbon could be identified by the increase of the transmittance signal after it reaches its minimum value (Chow et al., 2001; Sciare et al., 2003; Subramanian et al., 2006). Incomplete evolution of OC could be identified by the continuous decrease of the transmittance signal after the introduction of O₂ which suggests the continuous formation of PC despite the presence of O₂ (Schauer et al., 2003a). Accepted criteria about how to select the peak inert mode temperature are not available, making it a substantial challenge for the current thermal-optical method.

There are other factors that complicate the accurate measurement of carbonaceous aerosol, such as the ratio of converting organic carbon mass ($\mu\text{gC}/\text{m}^3$) to organic matter mass ($\mu\text{g}/\text{m}^3$) which is essential for the mass reconstruction studies (Andrews et al., 2000; Turpin and Lim, 2001). Resolving organic carbon into concentrations of specific organic compounds, which may provide valuable insights into its sources and effects (Zheng et al., 2002), is also of great interest. Another concern is the in-situ measurement of carbonaceous aerosol (such as the aerosol mass spectrometer, and the aerosol time-of-flight mass spectrometer) and its equivalence with the integrated results.

China is facing the challenge of serious air pollution, especially in Beijing, Shanghai and Pearl Delta (PRD) regions. Since 2003, there has been a rapid growth in the number of publications about air pollution in these regions (Chan and Yao, 2008). Though carbonaceous aerosol is a key constituent of air quality, sampling artifacts are not considered in most previous studies, thus introducing complexity and difficulty in direct comparison of carbonaceous aerosol across studies and regions. Moreover, nearly all the reported OC and EC concentration are obtained directly by the existing protocols, such as NIOSH and IMPROVE which were originally developed for the PM_{2.5} monitoring network in the United States. The inter-comparison of different protocols could provide important information about the thermal and optical properties of carbonaceous aerosol which greatly depend on its source (Schauer et al., 2003a; Hitzinger et al.,

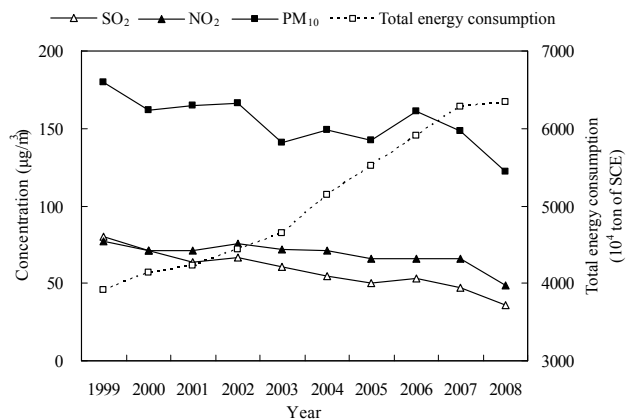


Fig. 1. Annual variation of SO₂, NO₂, PM₁₀ and total energy consumption in Beijing during the last decade from 1999 to 2008. SCE is Standard Coal Equivalent. Data from the Beijing Environment Bulletin, 1999 to 2008.

2006; Reisinger et al., 2008). However, few studies based on samples collected in China were available.

In this article, PM_{2.5} samples of Beijing, China were collected by a five channel sampler and subsequently analyzed by a thermal-optical method. Characteristics of the sampling artifact of Beijing carbonaceous aerosol, including its influence on the measured OC concentration and inter-comparison of different artifact elimination approaches, are presented. Results from the inter-comparison of thermal-optical methods, including the effects of charring correction method and peak inert mode temperature, are also shown.

2 Methods

2.1 Sampling site

Beijing is one of the world's largest mega cities. High levels of coal consumption, thousands of active construction sites, and a rapid increase in vehicle population have resulted in high emission of particulate matter and gaseous pollutants. The Beijing Municipal Government has implemented numerous air pollution control strategies since 2000, such as relocating heavy-polluting industrial facilities, implementing more stringent local emission standards for coal-fired boilers, and replacing older vehicle fleets with newer and cleaner ones (Wang et al., 2010). As a result, the annual average concentration of PM₁₀, SO₂ and NO₂ decreased gradually from 180, 80 and 77 $\mu\text{g}/\text{m}^3$ in 1999 to 122, 36 and 49 $\mu\text{g}/\text{m}^3$ in 2008, despite the rapid increase of total energy consumption (Fig. 1).

2.2 Sample collection

Ambient PM_{2.5} samples were collected by a Spiral Ambient Speciation Sampler (SASS, MetOne Inc.) at the Tsinghua

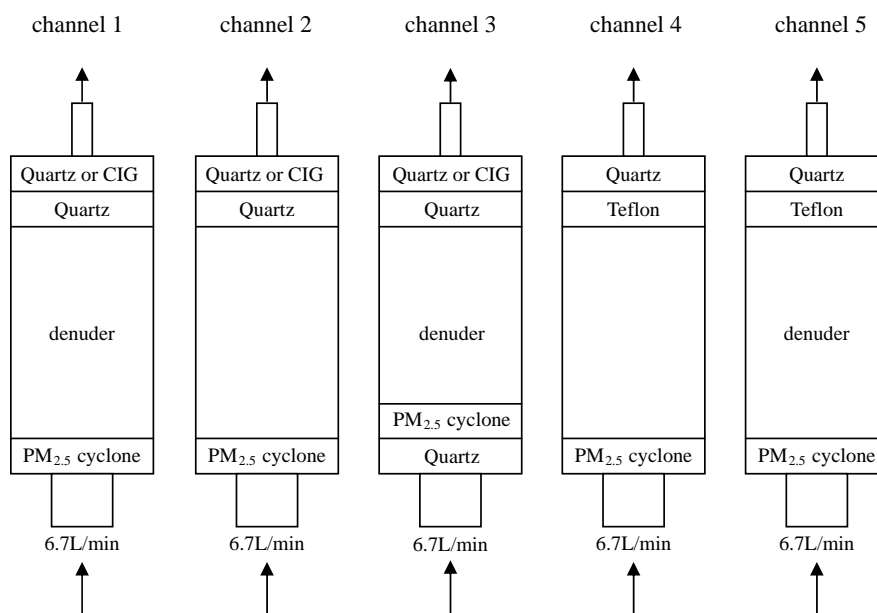


Fig. 2. Configuration of the SASS sampler. In the winter of 2009, all the five channels were operated; in the summer, channel 3 was not included during the sampling period, instead was run for 6 days after the sampling was finished; in the spring, only channel 1–3 were operated. The backup filter used in channel 1–3 was quartz in winter and summer, and was CIG in spring. See text for the purpose of different designs.

University campus in Beijing. The SASS sampler has five separate channels operated through a common controller and pump. Each channel contains a sharp cut cyclone designed to give a 2.5 μm cutpoint when operated at 6.7 L/min. Eighty-nine sets of daily samples were collected in 2009: 29 were collected from 9 January to 12 February (winter), 30 were collected from 9 April to 9 May (spring), and 30 were collected from 20 June to 20 July (summer). Configurations of the SASS sampler during each sampling period are shown in Fig. 2.

The winter and summer campaigns were designed to evaluate the characteristics of the positive sampling artifact of Beijing carbonaceous aerosol, including its value and the inter-comparison of different elimination approaches. The spring campaign was mainly aimed at the assessment of the negative artifact based on the activated carbon impregnated glass fiber (CIG) filter. Influence of the thermal-optical methods on the split of OC and EC was also evaluated. Loaded quartz filters from the three campaigns were used to evaluate the influence of charring correction method. Loaded quartz filters during the summer campaign were also used to assess the effects of the peak inert mode temperature.

The activated carbon denuder (provided by MetOne) is 20 mm long and 38 mm in diameter with about 1000, 1 mm² channels, inducing a typical residence time of 0.18 s at 6.7 L/min. A new denuder was used for each campaign. All filter used were 47 mm in diameter. The face velocity was 9.8 cm/s. The Teflon (R2PJ047) and quartz filters

(2500 QAT-UP) were from Pall Corp. (Ann Arbor, MI) and the CIG filters (1872-047) were from Whatman (Maidstone, England). All the quartz filters used throughout each campaign were taken from the same lot (Kirchstetter et al., 2001), and were pre-baked at 550 °C in air for 24 h (typically 2 days before each campaign). Thirty-four quartz filters were kept as blank. The average OC concentration of the blank filters was 0.44 $\mu\text{gC}/\text{m}^2$. All the data reported in this article were corrected by the filter blank concentration without special statement. Teflon and CIG filters were used as received from the manufacturers.

2.3 Sample analysis

The quartz and CIG filters were analyzed using a DRI Model 2001 thermal/optical carbon analyzer (Atmoslytic Inc., Calabasas, CA), which allows more accurate and precise control and monitoring of the sample temperature comparing with its previous version (Chow et al., 2005, 2007). Moreover, filter transmittance and reflectance are monitored simultaneously, providing an opportunity to compare the transmittance-defined EC (EC_T) and reflectance-defined EC (EC_R), since the uncertainties caused by the inter-equipment and inter-laboratory difference were minimized.

2.3.1 Analysis of quartz filter

The temperature protocols used for the analysis of quartz filters are shown in Table 1. The IMPROVE-A temperature

Table 1. Temperature protocols used in the present study.

step	gas	temperature (°C)				
		IMPROVE-A	He4-650	He4-700	He4-750	He4-800
1 (OC1)	He	140	140	140	140	140
2 (OC2)	He	280	280	280	280	280
3 (OC3)	He	480	480	480	480	480
4 (OC4)	He	580	650	700	750	800
5 (EC1)	O ₂ /He ^a	580	650–580 ^b	700–580 ^b	750–580 ^b	800–580 ^b
6 (EC2)	O ₂ /He ^a	740	740	740	740	740
7 (EC3)	O ₂ /He ^a	840	840	840	840	840

^a Actual gas composition: 98% He+2% O₂.

^b The temperature is reduced from that of OC4 stage to 580 °C.

protocol was the base case. The peak inert mode temperature (the temperature of He-4 stage) was increased from the 580 °C used in the IMPROVE-A protocol (IMPROVE-A protocol is also referred to as He4-580 protocol) to 650, 700, 750 and 800 °C respectively, yielding the four alternative temperature protocols referred to as He4-650, He4-700, He4-750 and He4-800. In the five protocols, EC_T is defined as the carbon that is measured after the filter transmittance returns to its initial value in the He/O₂ mode; EC_R is defined as the carbon measured after the filter reflectance returns to its initial value.

All of the quartz filters were analyzed by the IMPROVE-A protocol to determine the OC and EC concentration. EC_T and EC_R values were compared to evaluate the influence of charring correction method. Moreover, 10 pairs of denuded and un-denuded filters (front filter with particle loading in channel 1 and 2, respectively) collected during summer were also analyzed by the four alternative protocols to evaluate the effects of peak inert mode temperature.

In some protocols such as NIOSH 5040, the cool oven process (by turning off the oven heaters) was usually included at the end of the inert mode, since the temperature used for the determination of the last OC peak was higher than that used for the first EC peak. The cool oven process was included even in a protocol with the same temperature for the last OC peak and the first EC peak (Schauer et al., 2003a). However, due to the following factors, the cool oven process was not included in the four alternative protocols used in the present study. In many published thermograms (Chow et al., 2001, 2004; Schauer et al., 2003a; Sciare et al., 2003; Subramanian et al., 2006) with a wide range of peak inert mode temperature (from 550 to 900 °C), it could be found that the carbon signal (FID) was significantly above the base line and with a long “tail” at the end of the inert mode. If the cool oven process was applied, a considerable fraction of carbon would be evolved in it. Importantly, the amount of carbon evolved would depend on the characteristics of the cool oven process, such as the range and rate of temperature change. As a re-

sult, the cool oven process may complicate the comparison of temperature protocols which only differ with peak inert mode temperature, since the characteristics of the cool oven process may also influence the amount of carbon evolved in the inert mode. It should be pointed out that excluding the cool oven process would result in the confusion of different EC fractions, but it would not influence the total EC value which was the focus of the present study.

2.3.2 Analysis of CIG filter

Various temperature protocols have been used for the analysis of the CIG filter, which mainly differ with respect to (1) atmosphere of the analysis (i.e., He or N₂), and (2) maximum temperature up to which the CIG filter is heated. Since late 1990s, D. J. Eatough and co-workers have measured semi-volatile organic carbon in many American cities by the CIG filter in combination with a CIF (or BOSS) denuder. The CIG filters were analyzed in the N₂ atmosphere, and quite different maximum temperatures had been implemented, varying from 300 to 400 °C (Tang et al., 1994; Eatough et al., 2001, 2003). Subramanian et al. (2004) heated CIG filters up to 330 °C in the He atmosphere, whereas Mader et al. (2001) heated up to 450 °C. A significant concern during the CIG filter analysis is avoiding degradation of the filter material. Significant degradation at temperature of around 300 °C was reported by Modey et al. (2001). However, no evidence of degradation was found by Subramanian et al. (2004) and Grover et al. (2008a, b) who used 330 and 360 °C as the maximum temperature, respectively. The observed temperature difference at which degradation starts reflects the varied properties of the CIG filters used by the previous studies.

In the present study, CIG filters were analyzed in the He atmosphere, and three maximum temperature, 300, 250 and 200 °C, were tested. The analysis could not be completed when 300 °C was used, because of the large amount of organics that continuously evolved from the CIG filter due to the degradation of the filter material. The degradation was still significant when 250 °C was used, but was finally avoided

Table 2. Summary of the results from regression analysis.

<i>X</i> versus <i>Y</i>	<i>n</i>	<i>R</i> ²	Slope ^a	<i>X</i> average ^b	<i>Y</i> average ^b
OC _T versus OC _R (denuded)	89	0.9944	0.84	17.25	14.43
OC _T versus OC _R (undenuded)	89	0.9951	0.85	20.06	16.94
EC _T versus EC _R (denuded)	89	0.9031	1.78	3.81	6.62
EC _T versus EC _R (undenuded)	89	0.9025	1.86	3.73	6.84
<i>K</i> _{PC} of DQ versus <i>K</i> _{PC} of BQ (winter)	10	0.8901	1.21	0.95	1.20
<i>K</i> _{PC} of DQ versus <i>K</i> _{PC} of BQ (spring)	24	0.9692	1.24	1.49	1.84
<i>K</i> _{PC} of DQ versus <i>K</i> _{PC} of BQ (summer)	29	0.9514	1.31	1.56	2.01
OC _{DQ} versus OC _{BQ} –OC _{QBQ} (winter)	29	0.9954	1.037	32.57	34.20
OC _{DQ} versus OC _{BQ} –OC _{QBQ} (summer)	30	0.9066	1.098	8.77	9.82
OC _{DQ} versus OC _{BQ} –OC _{QBT} (winter)	29	0.9985	0.937	32.57	30.54
OC _{DQ} versus OC _{BQ} –OC _{QBT} (summer)	30	0.9583	0.882	8.77	7.72
OC _{DQ} versus OC _{BQ} –pos.OC _{QBT} (winter)	29	0.9974	0.965	32.57	31.52
OC _{DQ} versus OC _{BQ} –pos.OC _{QBT} (summer)	30	0.9569	0.918	8.77	8.05

^a Intercept was zero.

^b OC and EC values reported in µgC/m³.

when the maximum temperature was reduced to 200 °C. As a result, collected CIG filters were heated to 200 °C in the He atmosphere to determine the adsorbed organics.

3 Results and discussion

3.1 Inter-comparison of thermal-optical methods

3.1.1 Effects of the charring correction method

The influence of the charring correction method on the measured OC and EC concentration is shown in Fig. 3 and Table 2. All of the comparisons were made based on the results from the IMPROVE-A temperature protocol. Reflectance-defined OC (OC_R) and transmittance-defined OC (OC_T) correlated well with a slope of 0.85 and 0.84 for the bare quartz filter and denuded filter, respectively (Fig. 3a). A larger difference was seen for EC due to its relatively low concentration. Reflectance-defined EC (EC_R) was 1.86 and 1.78 times the concentration of transmittance-defined EC (EC_T), for the bare quartz filter and denuded filter, respectively (Fig. 3b). A similar slope of EC comparison was obtained for the urban, sub-urban, and IMPROVE network samples collected in the United States (1.78, calculated from the data reported by Chow et al., 2001).

All of the OC and EC concentrations reported below were defined by the transmittance correction without a special statement due to following factors. (1) The transmittance signal, that could reflect the process of PC formation and the evolution of light absorbing carbon (including both PC and native EC) throughout the filter thickness, was tracked to evaluate different temperature protocols. (2) A desire

to maintain consistency with previously published results (Cheng et al., 2009b).

3.1.2 Effects of different temperature protocols

Typical thermograms for a medium-loaded summer sample (TC=13 µgC/m³) obtained from the five protocols are shown in Fig. 4a to e. Operationally defined EC value, both defined by transmittance (EC_T) and reflectance (EC_R) correction, were found to continuously decrease with the peak inert mode temperature (Fig. 4f), inconsistent with Chow et al. (2004) who found EC_R was not influenced by the temperature protocol implemented.

The filter transmittance is tracked throughout the analysis to estimate the presence of possible artifacts that influences the split of OC and EC. When analyzed by the IMPROVE-A protocol, the filter transmittance reached its minimum value partway through the 580 °C temperature plateau in the inert mode and did not increase until the introduction of O₂ (Fig. 4 (a)), indicating PC was fully formed and premature evolution of light absorbing carbon was minimal. When the peak inert mode temperature was increased to 650 °C, the transmittance signal started to increase at the end of the inert mode (Fig. 4b), indicating the loss of light absorbing carbon. All of the 10 pair of samples (denuded and un-denuded) exhibited a similar loss which began with the He4-650 protocol. The extent of the light absorbing carbon premature evolution could be estimated by *K*_{loss}, which is defined as:

$$K_{\text{loss}} = \ln\left(\frac{T_{\text{end}}}{T_{\text{min}}}\right) \quad (1)$$

where *T*_{end} is the filter transmittance at the end of inert mode and *T*_{min} is its minimum value. *K*_{loss} is the attenuation

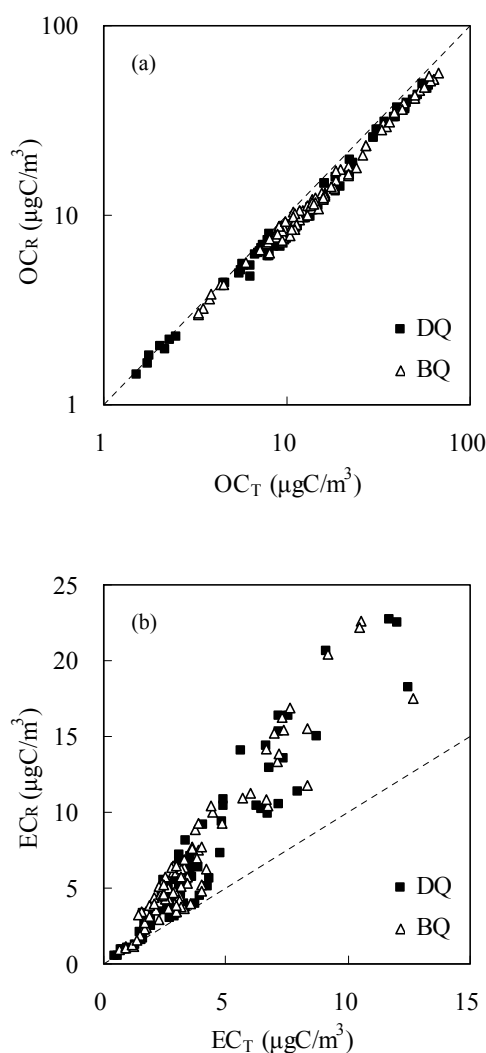


Fig. 3. Comparison of (a) transmittance-defined OC (OC_T) and reflectance-defined OC (OC_R) and (b) transmittance-defined EC (EC_T) and reflectance-defined EC (EC_R). Results were obtained from IMPROVE-A temperature protocol (He4-580 protocol). Results from parallel denuded (DQ) and undenuded (BQ) quartz filters are shown separately.

caused by the evolution of light absorbing carbon in the inert mode. $K_{\text{loss}}=0$ indicates no loss of light absorbing carbon; $K_{\text{loss}}>0$ indicates the presence of loss, and its amount increases with K_{loss} . It should be pointed out that K_{loss} is meaningless if the transmittance signal continues to drop in the inert mode. As shown in Fig. 4f, loss of light absorbing carbon increased with the peak inert mode temperature (from 650 to 800 °C), which could also be demonstrated by Fig. 4b to e. Within the five protocols, only the IMPROVE-A protocol could avoid the premature evolution of light absorbing carbon; moreover, no evidence for the incomplete evolution of OC was observed.

Although there was premature evolution of light absorbing carbon with the He4-650 protocol, the filter transmittance was still below its initial value at the end of the inert mode. As a result, the OC/EC split still occurred in the He/O₂ mode. But when the peak inert mode temperature was increased to 800 °C, the filter transmittance exceeded its initial value before the introduction of O₂ for nine (of the ten) denuded samples, and for six (of the ten) un-denuded samples, respectively. This was referred to as “early split” by Chow et al. (2004). It seems that “early split” occurs at lower temperature for Beijing carbonaceous aerosol compared with other regions such as North America and Europe. For example, “early split” occurred in 40% of un-denuded Fresno samples using a protocol with a peak inert mode temperature of 900 °C (Chow et al., 2004); when using the NIOSH protocol (the peak inert mode temperature is 870 °C), the OC/EC split occurred in the He/O₂ mode for all the denuded and un-denuded samples collected in Pittsburgh (Subramanian et al., 2006), and for the un-denuded Bakersfield (Schauer et al., 2003a) and Crete (Greece) samples (Sciare et al., 2003).

Moreover, in all of the thermograms obtained by the He4-800 protocol (Fig. 4e; see Supplement for more examples), the last OC peak was characterized by the overlapping of two separate peaks, indicating evolution of two carbon fractions with different thermal stability. The first peak was the carbon evolved when the temperature was increased from 480 to 800 °C, whereas the second was the carbon evolved during the 800 °C plateau. The overlapping could not be detected in any of the published thermograms of samples from North America and Europe (Chow et al., 2001, 2004; Schauer et al., 2003a; Sciare et al., 2003; Subramanian et al., 2006) even if the peak inert mode temperature used was close to 900 °C. Thus, the overlapping is a unique phenomenon which has only been found in Beijing aerosol.

In addition, the discrepancy between EC values defined by different temperature protocols was larger for Beijing carbonaceous aerosol. The ratio of He4-580 EC (EC value defined by the He4-580 protocol; similar hereinafter) to He4-800 EC averaged at 1.86 and 1.98 for un-denuded and denuded Beijing samples respectively, whereas the ratio of He4-550 EC to He4-870 EC was only about 1.5 or even lower for ambient samples collected in North America and Europe (Table 3). With respect to the source samples, the EC concentration of the wood smoke sample was significantly influenced by the protocol implemented, while the EC concentration of the carbon black and coal fly ash remained nearly constant despite analyzed by different protocols (Table 3). Importantly, as shown in Table 3, the He4-580 EC to He4-800 EC ratio of Beijing ambient samples was only a little lower than the He4-550 EC to He4-870 EC ratio of the wood smoke sample which was characterized by a high concentration of brown carbon.

Brown carbon as a light absorbing component has recently come into the forefront of atmospheric research (Andreae and Gelencsér, 2006; Lukács, et al., 2007). The light

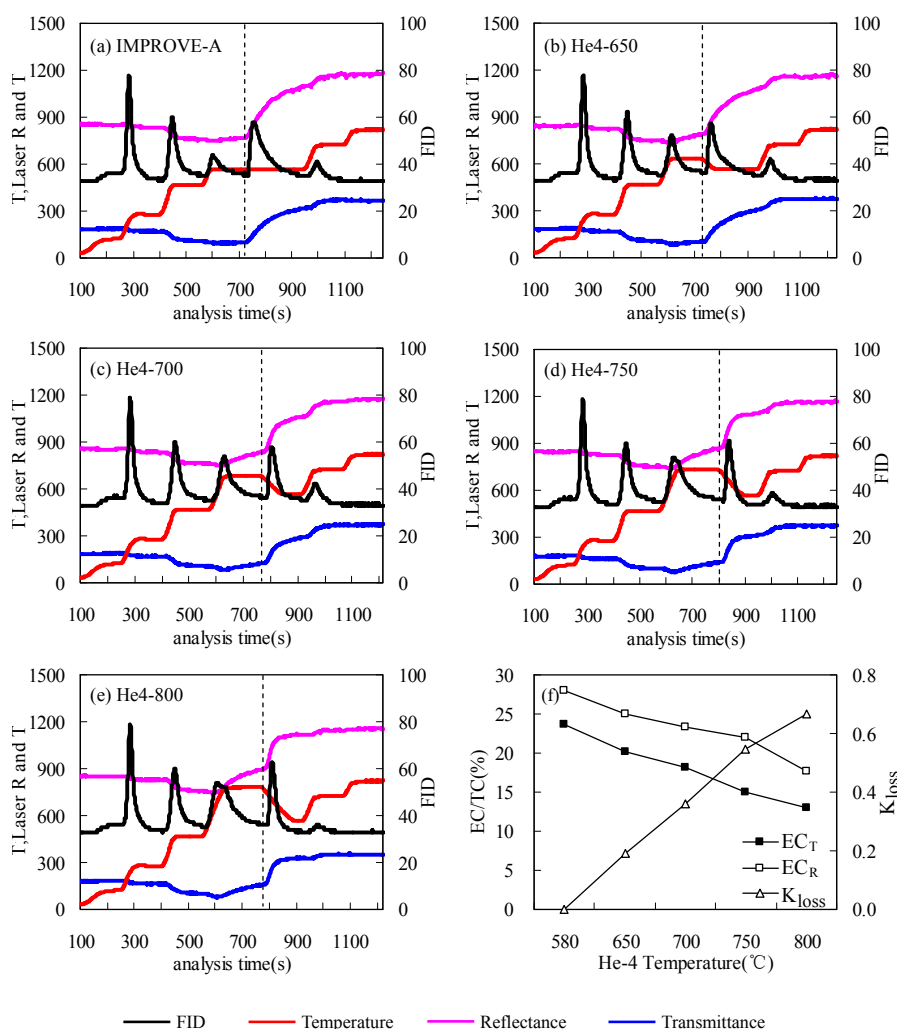


Fig. 4. Typical thermograms for a medium-loaded summer sample ($TC=13\ \mu\text{gC}/\text{m}^3$) obtained from the five protocols (a–e), with the dash line indicating the introduction of O₂. Influence of peak inert mode temperature (He-4 temperature) on EC values defined by transmittance (EC_T) and reflectance (EC_R) correction, and on loss of light absorbing carbon (K_{loss}) is shown in (f).

absorption coefficient of brown carbon increases strongly from long to short wavelengths, resulting in its brown appearance (Alexander et al., 2008). The “tar balls”, which have been widely observed in Africa, Europe and North America (Pósfai, et al., 2004; Hand et al., 2005), are considered as an important type of brown carbon. Though both types can absorb light, “tar balls” differs substantially from black carbon in terms of morphology. “Tar balls” are large, amorphous, and predominantly isolated carbon spheres (diameter of 100 to 400 nm), whereas soot consists of aggregates of spherules mostly 20 to 50 nm in diameter (van Poppel et al., 2005). The integrating sphere method (Wonaschütz, et al., 2009) originally developed by Heintzenberg (1982) is an effective approach to separate brown carbon from soot, based on their different wavelength dependence of light absorption characteristics. As shown by recent studies using the inte-

grating sphere method, brown carbon was strongly linked to biomass burning (Reisinger et al., 2008; Wonaschütz et al., 2009). Kirchstetter et al. (2004) also demonstrated that low-temperature, incomplete combustion processes, including biomass burning, could produce light absorbing aerosols that exhibited much stronger spectral dependence than high temperature combustion processes, such as diesel combustion. Moreover, the discrepancy between EC values determined by different thermal and thermal-optical methods was found to be larger when the concentration of brown carbon was high (Reisinger et al., 2008), while all methods gave comparable EC concentration when diesel traffic was the major source of EC (Hitzenberger et al., 2006). As a result, it is reasonable to conclude that Beijing aerosol has a much higher concentration of brown carbon compared with North America and Europe, due to its much larger discrepancy

Table 3. Ratios of EC value determined by different temperature protocols.

Ratio definition ^a	Value	Sampling site	Sample description	Reference
He4-580/He4-800	1.86/ 1.98 ^b	Beijing, China	Jun; ambient	this study
He4-580/He4-900	1.3 ^c	Fresno, CA	Aug–Sep; ambient	Chow et al., 2009
He4-550/He4-870	1.5 ^c	Vienna, Austria	Feb–Mar; ambient	Reisinger et al., 2008
He4-550/He4-870	1.5 ^c	Bakersfield, CA	Dec; ambient	Schauer et al., 2003a
He4-550/He4-870	1.5 ^c	St. Louis, IL	Apr; ambient	Schauer et al., 2003a
He4-550/He4-870	1.2 ^c	Crete, Greece	long term; ambient	Sciare et al., 2008
He4-550/He4-870	2.16 ^c	–	wood smoke; source	Schauer et al., 2003a
He4-550/He4-870	1.09 ^c	–	coal fly ash; source	Schauer et al., 2003a
He4-550/He4-870	1.00 ^c	–	carbon black; source	Schauer et al., 2003a

^a Temperature protocols were defined by the peak inert mode temperature.

^b See text for details.

^c Ratios calculated from published data.

between EC values defined by different temperature protocols that was almost comparable with that of the wood smoke sample. The evolution of brown carbon at high temperature (such as 800 °C) in the inert mode is the most likely factor that caused “early split” occurring at relatively low temperature for Beijing aerosol.

3.2 Characteristics of sampling artifacts

3.2.1 Evaluation of the organic denuder

The possibility of additional artifacts caused by the application of an organic denuder should be excluded first. As suggested by Cheng et al. (2009a, b), four factors should be considered:

The first is the denuder breakthrough and efficiency. Denuder breakthrough, defined as the amount of gaseous organics that are not removed by the denuder and subsequently adsorbed by the filter downstream, was determined by channel 3 (Fig. 2), which was usually referred to as the “breakthrough channel”. In channel 3, particles were removed by the quartz filter placed upstream of the PM_{2.5} cyclone, and gaseous organics were captured by the organic denuder. As a result, OC collected by the filter pack downstream of the denuder was from breakthrough. Only breakthrough that can be adsorbed by quartz filter is discussed here, while breakthrough that can be adsorbed by CIG filter is discussed separately in Sect. 3.2.4. As shown in Fig. 5, breakthrough OC (averaging 0.39 μgC/m²) was comparable with the filter blank values, indicating that the efficiency of the activated carbon denuder to remove the positive artifact was 100% during each sampling campaign.

The second factor is the particles loss due to the diffusion to the walls of the denuder, which may be evaluated by comparing the EC concentrations of denuded (EC_{DQ}) and bare (EC_{BQ}) quartz filter (Ding et al., 2002). As shown in Fig. 5, EC_{DQ} compared well with EC_{BQ}. Paired-t testing

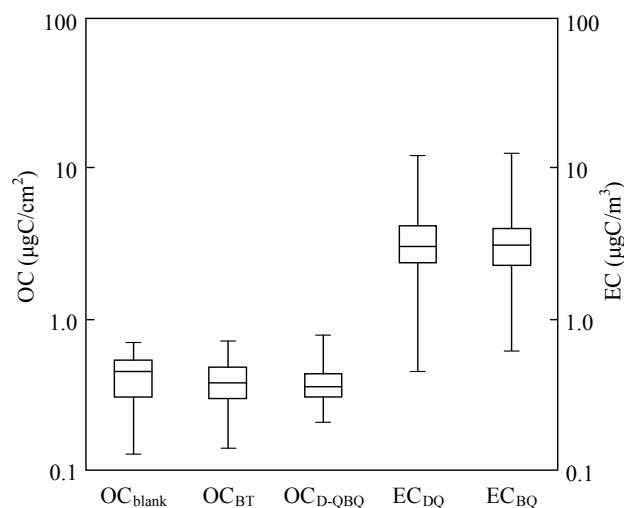


Fig. 5. Concentration of filter blank (OC_{blank}), denuder breakthrough (OC_{BT}), and OC measured by denuded backup quartz filter (OC_{D-QBQ}); EC concentrations measured by denuded (EC_{DQ}) and undenuded (EC_{BQ}) quartz filter are also shown. The boundary of the box closest to 0.1 indicates the 25th percentile, the line within the box marks the median, and the boundary of the box farthest from 0.1 indicates the 75th percentile, whiskers above and below the box indicate the maximum and minimum.

also showed they were not significantly different at a 95% level of confidence.

The third is the evaporation of particulate organic carbon during transportation through the denuder, which could be minimized if the residence time of particles in the denuder is less than 0.2 s (Strommen and Kamens, 1999; Mader et al., 2001). The residence time in the denuder used in the present study was 0.18 s, indicating that off-gassing of particulate organic carbon should be minimal.

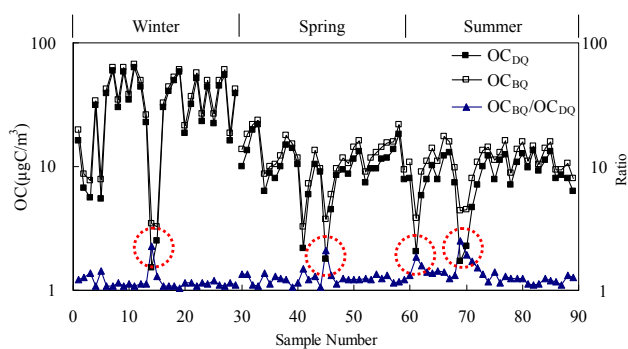


Fig. 6. Comparison of OC concentration determined by denuded (OC_{DQ}) and undenuded (OC_{BQ}) quartz filter. The ratio of OC_{BQ} to OC_{DQ} (OC_{BQ}/OC_{DQ}) is also shown. The peak of OC_{BQ} to OC_{DQ} ratio is marked by the red-dotted cycle.

The fourth is the shedding of the denuder material (activated carbon), or the contamination of EC (Subramanian et al., 2004; Viana et al., 2006a). No tiny charcoal particles were observed on the denuded filters, both quartz and Teflon, throughout the whole sampling period. Moreover, the result of the OC/EC analysis showed that no EC was detected on the front quartz filter in the breakthrough channel (channel 3), demonstrating the contamination of EC was negligible.

3.2.2 The positive artifact

OC concentration determined by the bare quartz filter in channel 2 (OC_{BQ}) and by the denuded quartz filter in channel 1 (OC_{DQ}) during the whole sampling period were compared in Fig. 6. The positive artifact was defined as the difference between OC_{BQ} and OC_{DQ} . Positive artifact averaged 3.56, 2.26 and 2.61 $\mu\text{gC}/\text{m}^3$, and constituted 10%, 18% and 23% of OC_{BQ} , during winter, spring and summer respectively. The ratio of OC_{BQ} to OC_{DQ} is also shown in Fig. 6, which was significantly high when the organic carbon concentration was low.

The positive artifact of Beijing carbonaceous aerosol was compared with results from other regions, including North America and Europe, in Fig. 7. The positive artifact in Beijing, both the value and its fraction in OC_{BQ} , was comparable with other regions. The fraction of positive artifact in OC_{BQ} was considerable (typically above 30%) when the concentration of organic carbon was low, such as the results from Toronto, Vancouver, Ghent and Barcelona. In addition, a substantial amount of OC_{BQ} was from the positive artifact (about 50%) when the influence of biomass burning was important. Results from low-volume indoor sampling are also shown in Fig. 7, and the fraction of positive artifact in OC_{BQ} (above 60%) was found to be more significant than ambient results.

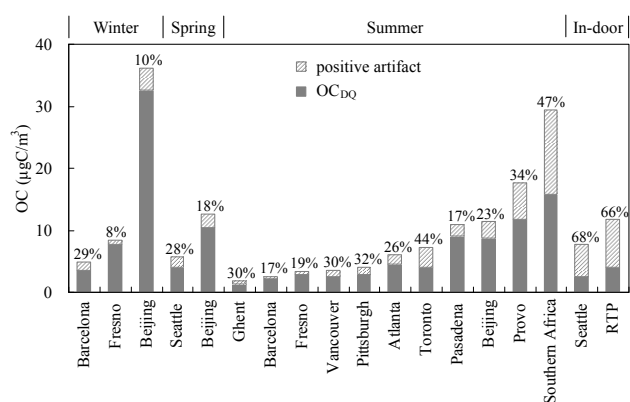


Fig. 7. Comparison of positive artifact of Beijing carbonaceous aerosol with other regions. Results from low-volume in-door sampling are also shown. Positive artifact was calculated as the difference between OC measured by bare (OC_{BQ}) and denuded (OC_{DQ}) quartz filter. The percentage is the fraction of positive artifact in OC_{BQ} . Data from Viana et al., 2006b (Barcelona, Spain), Chow et al., 2006 (Fresno, CA), Lewtas et al., 2001 (Seattle, WA), Viana et al., 2006a (Ghent, Belgium), Fan et al., 2004 (Vancouver, Canada), Cabada et al., 2004 (Pittsburgh, PA), Solomon et al., 2003 (Atlanta, GA), Fan et al., 2003 (Toronto, Canada), Mader et al., 2001 (Pasadena, CA), Ding et al., 2002 (Provo, UT), Eatough et al., 2003 (southern Africa), Pang et al., 2002 (Seattle, WA; in-door) and Olson and Norris, 2005 (Research Triangle Park (RTP), NC; in-door).

Figure 8 presented the average of the carbon evolution pattern of bare (BQ) and denuded (DQ) quartz filter from the winter and summer campaigns respectively. Significantly different patterns were observed for winter and summer samples. For winter samples, the carbon evolution pattern of BQ and DQ mainly differed with the OC1 fraction. The BQ to DQ ratio of the average concentration of OC1 fraction was 1.31, whereas the ratios of the other fractions were close to 1.0 (below 1.05) (Fig. 8a), indicating that nearly all of the adsorbed gaseous organics would evolve off the filter when heated to 140 °C in the He atmosphere during the thermal-optical analysis. However, for summer samples (Fig. 8b), the BQ to DQ ratio of all the four OC peaks (OC1 to OC4) were significantly higher than 1.0 (above 1.10). It is unlikely that originally gaseous organics could be retained on the quartz filter at a temperature above 200 °C (Grover et al., 2008a, b; Fan et al., 2003, 2004). As a result, the most probable explanation is that adsorbed gaseous organics undergo reactions with air oxidants (such as ozone and nitrogen oxides) on the bare quartz filter during sampling, which has been referred to as the reaction artifact. Previous studies mainly focused on the reaction or degradation of polycyclic aromatic hydrocarbons (PAH) on filters. Several types of oxidant denuders have been used for this purpose, such as the activated carbon denuder (Schauer et al., 2003b), KNO_2 denuder (Tsapakis and Stephanou, 2003), KI denuder (Possanzini et al., 2006), and MnO_2 denuder (Liu et al., 2006). Schauer et al. (2003b)

found that substantial degradation of benzo[a]pyrene (BaP) and other 5- and 6-ring PAH could occur during sampling, which showed a near-linear dependence on ozone concentration. For the samples collected at high ozone levels (about 80 ppb), the PAH concentration was underestimated by 50% (Schauer et al., 2003b). Menichini (2009) also showed that the on-filter loss of BaP was typically in the 20–55% range. The oxidant products of PAH include oxygenated and nitrated PAH (OPAH and NPAH, respectively). Importantly, Goldfarb and Suuberg (2008) demonstrated that the addition of aldehyde, carboxyl, and nitro groups on to PAH would increase the enthalpy of sublimation and decrease the vapor pressure compared with the parent PAH. Summertime Beijing is characterized by the high concentration of ozone. For example, as reported by Lin et al. (2009), during an ozone episode in July, the daily mean concentrations were between 50 and 100 ppb with an average of 70 ppb, and the 8-h average concentrations were between 56 and 144 ppb with an average of 109 ppb. Moreover, the ozone concentration in the lower troposphere over Beijing shows an increasing trend during the last decade (Ding et al., 2008; Tang et al., 2009). As a result, oxidation of gaseous organics adsorbed by the bare quartz filter was expected to be considerable during summertime. The oxygenated and nitrated derivatives of the adsorbed organics which have higher thermal stability are the most likely cause of the distinct carbon evolution pattern of summer samples.

Chow et al. (2004) suggested that the positive artifact would have considerable influence on the thermal-optical split of OC and EC, since charring of the adsorbed gaseous organics might account for a substantial fraction of the PC formed during the inert mode of the analysis. The amount of PC could be estimated by the attenuation caused by its formation, K_{PC} , which is defined as:

$$K_{PC} = \ln\left(\frac{T_{\text{initial}}}{T_{\text{min}}}\right) \quad (2)$$

where T_{min} and T_{initial} are the minimum and initial value of the filter transmittance, respectively. PC formed on the bare quartz filter could be apportioned to the charring of adsorbed gaseous organics and the charring of particulate OC, by comparing K_{PC} of denuded (DQ) and undenuded (BQ) quartz filters. For this purpose, the minimum transmittance should be detectable for both BQ and DQ, which was met by 10, 24 and 29 pair of samples collected during winter, spring and summer respectively. The charring of adsorbed gaseous organics accounted for 21%, 24% and 31% of PC formed on the bare quartz filter (Table 2), whereas the positive artifact constituted 10%, 18% and 23% of OC determined by the bare quartz filter (OC_{BQ}), during winter, spring and summer respectively. As a result, the PC formation potential of adsorbed gaseous organics was higher than that of particulate OC.

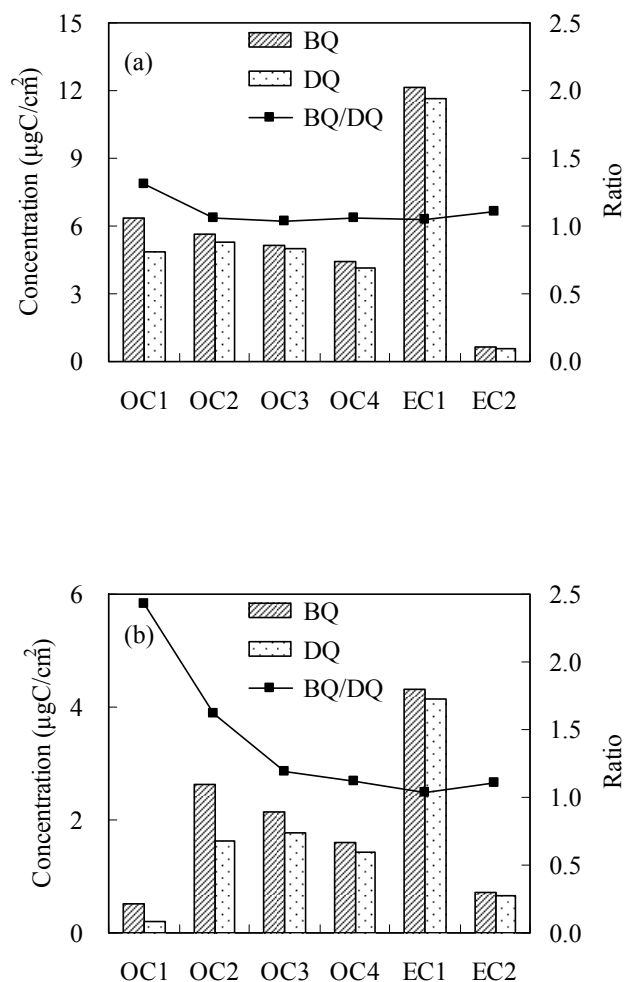


Fig. 8. Average concentration of carbon evolving at each temperature step. (a) results from denuded (DQ) and undenuded (BQ) quartz filters collected during winter; (b) results from summer samples. BQ to DQ ratio of each carbon fraction (BQ/DQ) is also shown.

3.2.3 Evaluation of the backup quartz approach

The backup quartz approach, in which a backup quartz filter is placed either behind a front quartz filter (QBQ, quartz-quartz in series method) or in a parallel port behind a Teflon filter (QBT, Teflon-quartz in series method), has been complicated by the origin of backup OC (OC collected by the backup filter, either QBQ or QBT) for years (Turpin et al., 2000). The denuder approach, in which organic denuder is used in combination with a backup filter, can separate the adsorption and volatilization process. As a result, origin of the backup OC may be directly and quantitatively evaluated by the inter-comparison of the denuder approach and the backup quartz approach, which could also provide deep insight into the positive sampling artifact problem. The denuder-based apportionment method for the determination

of the origin of backup OC was developed by Cheng et al. (2009a), and assumed that: (1) backup OC consists of both gaseous organics passing through the front filter (positive artifact-contributed) and volatilized particulate organic carbon (negative artifact-contributed); (2) OC determined by the denuded backup quartz filter, after corrected for breakthrough, provides an upper limit of the negative artifact-contributed OC; (3) the positive artifact-contributed OC is calculated as the difference between the backup OC and the negative artifact-contributed OC. Apportionment results from the winter and summer campaign are briefly presented below. See Cheng et al. (2009b) for a detailed discussion based on the winter samples.

(1) The quartz-quartz in series method. During winter and summer, OC collected by the denuded backup quartz filter in channel 1, OC_{D-QBQ} (averaging $0.39 \mu\text{gC}/\text{cm}^2$), was comparable with filter blanks (Fig. 5), indicating that no volatilized OC was collected. As a result, all of the OC collected by QBQ (OC_{QBQ} , in channel 2) was from positive artifact. Therefore, the quartz-quartz in series method was reliable for assessing the positive artifact. However, as demonstrated by the linear regression results (Table 2), QBQ adsorbed less gaseous organics than the front bare quartz filter due to the relatively small sampling volume (typically 9.3 m^3). Thus, the quartz-quartz in series method overestimated the OC concentration by 3.7% and 9.8%, during winter and summer respectively (Table 2).

(2) The Teflon-quartz in series method. OC collected by the denuded backup quartz filter in channel 5 (denuded-QBT) averaged 0.98 and $0.32 \mu\text{gC}/\text{m}^3$, and constituted 18% and 9% of OC collected by QBT (OC_{QBT}), during winter and summer respectively, indicating a substantial amount of OC_{QBT} was from the negative artifact. Therefore, the Teflon-quartz in series method underestimated the OC concentration by 6.3% and 11.8%, during winter and summer respectively (Table 2). Moreover, even using the positive artifact-contributed OC_{QBT} (pos. OC_{QBT}) for correction, the OC concentration was still underestimated by 3.5% and 8.2%, during winter and summer respectively (Table 2). Cheng et al. (2009b) suggested this was caused by the difference in the adsorption properties of the loaded filter (front quartz filter in channel 2) and the filter without particle loading (QBT).

3.2.4 The negative artifact

As discussed in Sect. 2.3.2, the maximum temperature (200°) used for the analysis of CIG backup filters, which were collected during the spring, is much lower compared with previous studies (from 300 to 450°C). Grover et al. (2008a, b) suggested that organics evolved from the CIG filter below 200°C were originally gaseous organics, whereas organics evolved between 250 to 350°C were volatilized particulate OC (semi-volatile OC, SVOC). Similar definitions were adopted by Fan et al. (2003, 2004) for the analysis of the XAD impregnated quartz filter. It should be pointed out

that properties of the CIG filter used by different studies (including the present) seem to be variant. As a result, the origin of OC measured by the CIG filter (OC_{CIG}) in this study, whether originally gaseous organics or volatilized particulate OC (SVOC), is difficult to determine only based on the temperature protocol.

Significant OC was measured on the CIG filter in the breakthrough channel (channel 3) during the spring campaign, averaging $19.64 \mu\text{gC}/\text{m}^3$, which undoubtedly was from originally gaseous organics not removed by the denuder, or breakthrough. Comparable OC was measured by the denuded backup CIG filter in channel 1, averaging $18.37 \mu\text{gC}/\text{m}^3$, which should be the sum of SVOC and breakthrough. It is unlikely that the concentration of SVOC that could be adsorbed by the CIG filter was zero. As a result, the most likely explanation is that the OC_{CIG} determined in this study is from originally gaseous organics, indicating the maximum temperature used (200°C) is not high enough for the determination of SVOC. However, the maximum temperature could not be increased further or the degradation of filter material would occur, indicating that the CIG filter used in this study was not suitable for the analysis of SVOC.

The average value of OC_{CIG} measured by the CIG filter placed behind the bare quartz filter (in channel 2) was $27.11 \mu\text{gC}/\text{m}^3$, which was the total concentration of gaseous organics that could be adsorbed by CIG filter (or sensitive to CIG filter). Thus only a relatively small fraction of originally gaseous organics ($7.47 \mu\text{gC}/\text{m}^3$, calculated as the difference between the total concentration and breakthrough) was removed by the denuder, indicating the denuder efficiency for removing gaseous organics sensitive to the CIG filter was only about 30%.

The sampling configuration that uses an activated carbon denuder in combination with a CIG backup filter has been demonstrated as reliable in the United States. However, it has not been evaluated in China before this study, and whether it is suitable for China remains inconclusive. The high concentration of total gaseous organics sensitive to CIG filter presents a substantial challenge. The concentration encountered during the spring campaign ($27.11 \mu\text{gC}/\text{m}^3$) was about twice as high as that reported by Lewtas et al. (2001) ($13 \mu\text{gC}/\text{m}^3$, results from Seattle, WA during the spring). A common approach to improve the denuder efficiency is to increase the area of adsorption surface (typically increase the length of a denuder with a given cross area, Fan et al., 2003), which would also increase the residence time of particles in the denuder. In the present study, the residence time in the denuder was 0.18 s , already very close to 0.2 s , a suggested value to minimize off-gassing of particulate organic carbon during transportation through the denuder (Strommen and Kamens, 1999; Mader et al., 2001), indicating the denuder length could not be increased further. As a result, the CIG filter seemed unsuitable for the measurement of SVOC based on the denuder used in this study, due to the variety in the properties of the CIG filter especially the temperature

at which degradation of filter material starts, and also due to the low denuder efficiency for removing gaseous organics sensitive to CIG filter.

4 Conclusions

The positive sampling artifact of Beijing carbonaceous aerosol was evaluated by both the denuder approach and the backup quartz approach. Adsorbed gaseous organics constituted 10% and 23% of OC concentration determined by the bare quartz filter (OC_{BQ}) during winter and summer respectively. The positive artifact in Beijing, both the value and the fraction in OC_{BQ} , was comparable with other regions such as North America and Europe. For winter samples, nearly all of the adsorbed gaseous organics would evolve off the filter within the OC1 stage when analyzed by the IMPROVE-A protocol. However, for summer samples, the adsorbed gaseous organics were found to continuously evolve off the filter during the whole inert mode (OC1 to OC4 stage), perhaps due to the oxidation of the adsorbed organics during sampling (reaction artifact) which would increase their thermal stability. The quartz-quartz (QBQ) in series method was demonstrated to be more reliable than the Teflon-quartz (QBT) in series method for assessing the positive artifact, since all of the OC collected by QBQ was from originally gaseous organics whereas a substantial amount of OC collected by QBT was from volatilized particulate OC.

The negative artifact was also evaluated. OC concentration detected on the denuded backup quartz filter was comparable with filter blank values during the winter and summer campaign, indicating that the amount of volatilized particulate OC that could be adsorbed by quartz filter was negligible. The CIG filter was tested as the backup filter during the spring campaign. Only about 30% of originally gaseous organics that could be adsorbed by the CIG filter was removed by the activated carbon denuder used in this study. Moreover, properties of the CIG filters used by different studies (including the present), especially the temperature at which degradation of filter material starts, seem to be variant. As a result, it seems that the CIG filter might not be suitable for the assessment of negative artifact in China.

Charring correction methods was shown to have significant influence on the thermal-optical split of OC and EC. When analyzed by the IMPROVE-A protocol, the reflectance-defined EC value was about twice as high as that defined by transmittance.

Influence of the peak inert mode temperature was evaluated based on the summer samples. The following thermal-optical characteristics of Beijing carbonaceous aerosol were drawn from the intercomparison. (1) The EC value, both defined by transmittance and reflectance correction, was found to continuously decrease with the peak inert mode temperature. (2) Premature evolution of light absorbing carbon began when the peak inert mode temperature was increased from

580 to 650 °C; when further increased to 800 °C, the filter transmittance frequently exceeded its initial value before the introduction of O₂, which was called “early split”. Moreover, it was shown that “early split” occurred at lower temperature for Beijing carbonaceous aerosol compared with other regions such as North America and Europe. (3) When the peak inert mode temperature was increased to 800°, the last OC peak was characterized by the overlapping of two separate peaks. The overlapping is a unique phenomenon which has only been found in Beijing aerosol. (4) The discrepancy between EC values defined by different temperature protocols was larger for Beijing carbonaceous aerosol compared with North America and Europe, perhaps due to higher concentration of brown carbon in Beijing aerosol.

Appendix A

DQ:	denuded quartz filter
BQ:	un-denuded (bare) quartz filter
CIG:	activated carbon impregnated glass fiber filter
OBQ:	backup quartz filter placed behind a front quartz filter
QBT:	backup quartz filter placed behind a front Teflon filter
OC_{DQ} :	OC concentration measured by the denuded quartz filter
OC_{BQ} :	OC concentration measured by the un-denuded quartz filter
OC_{QBQ} :	OC concentration measured by the backup quartz filter placed behind a front quartz filter
OC_{BQT} :	OC concentration measured by the backup quartz filter placed behind a front Teflon filter
OC_{CIG} :	OC concentration measured by the activated carbon impregnated glass fiber filter
EC_{DQ} :	EC concentration measured by the denuded quartz filter
EC_{BQ} :	EC concentration measured by the un-denuded quartz filter
OC_R :	OC value defined by the reflectance charring correction method
OC_T :	OC value defined by the transmittance charring correction method
EC_R :	EC value defined by the reflectance charring correction method
EC_T :	EC value defined by the transmittance charring correction method

Acknowledgements. This work was supported by the National Natural Science Foundation of China through grant number 20625722 to He Kebin, and by the Foundation for the Author of National Excellent Doctoral Dissertation of PR China to Duan Fengkui (2007B57). The authors would like to acknowledge visiting scholar Charles N. Freed for revising the paper. The authors would also like to acknowledge Chen Lai-guo in South China Institute of Environmental Science, MEP for his help in the OC/EC analysis.

Edited by: A. Petzold

References

- Andreae, M. O. and Gelencsér, A.: Black carbon or brown carbon? The nature of light-absorbing carbonaceous aerosols, *Atmos. Chem. Phys.*, 6, 3131–3148, doi:10.5194/acp-6-3131-2006, 2006.
- Andrews, E., Saxena, P., Musarra, S., Hildemann, L. M., Koutrakis, P., McMurry, P. H., Olmez, I., and White, W. H.: Concentration and composition of atmospheric aerosols from the 1995 SEAVS Experiment and a review of the closure between chemical and gravimetric measurements, *J. Air Waste Manage. Assoc.*, 50, 648–664, 2000.
- Alexander, D. T. L., Crozier, P. A., and Anderson, J. R.: Brown carbon spheres in East Asian outflow and their optical properties, *Science*, 321, 833–836, 2008.
- Cabada, J. C., Pandis, S. N., Subramanian, R., Robinson, A. L., Polidori, A., and Turpin, B.: Estimating the secondary organic aerosol contribution to PM_{2.5} using the EC tracer method, *Aerosol Sci. Technol.*, 38, 140–155, 2004.
- Cadle, S. H., Groblicki, P. J., and Mulawa, P. A.: Problems in the sampling and analysis of carbon particulate, *Atmos. Environ.*, 17, 593–600, 1983.
- Chan, C. K. and Yao, X. H.: Air pollution in mega cities in China, *Atmos. Environ.*, 42, 1–42, 2009.
- Cheng, Y., He, K. B., Duan, F. K., Zheng, M., Ma, Y. L., and Tan J. H.: Measurement of semivolatile carbonaceous aerosols and its implications: a review, *Environ. Int.*, 35, 674–681, 2009a.
- Cheng, Y., He, K. B., Duan, F. K., Zheng, M., Ma, Y. L., and Tan, J. H.: Positive sampling artifact of carbonaceous aerosols and its influence on the thermal-optical split of OC/EC, *Atmos. Chem. Phys.*, 9, 7243–7256, doi:10.5194/acp-9-7243-2009, 2009b.
- Chow, J. C., Watson, J. G., Crow, D., Lowenthal, D. H., and Merrifield, T.: Comparison of IMPROVE and NIOSH carbon measurements, *Aerosol Sci. Technol.*, 34, 23–34, 2001.
- Chow, J. C., Watson, J. G., Chen, L. A., Arnott, W. P., and Moosmüller, H.: Equivalence of elemental carbon by thermal/optical reflectance and transmittance with different temperature protocols, *Environ. Sci. Technol.*, 38, 4414–4422, 2004.
- Chow, J. C., Watson, J. G., Chen, L.-W. A., Paredes-Miranda, G., Chang, M.-C. O., Trimble, D., Fung, K. K., Zhang, H., and Zhen Yu, J.: Refining temperature measures in thermal/optical carbon analysis, *Atmos. Chem. Phys.*, 5, 2961–2972, doi:10.5194/acp-5-2961-2005, 2005.
- Chow, J. C., Watson, J. G., Lowenthal, D. H., Chen, L. A., and Magliano, K. L.: Particulate carbon measurements in California's San Joaquin Valley, *Chemosphere*, 62, 337–348, 2006.
- Chow, J. C., Watson, J. G., Chen, L. A., Chang, M. O., Robinson, N. F., Trimble, D., and Kohl, S.: The IMPROVE-A temperature protocol for thermal/optical carbon analysis: maintaining consistency with a long-term database, *J. Air Waste Manage. Assoc.*, 57, 1014–1023, 2007.
- Chow, C. J., Watson, J. G., Doraiswamy, P., Chen, L. A., Sodeman, D. A., Lowenthal, D. H., Park, K., Arnott, W. P., and Motallebi, N.: Aerosol light absorption, black carbon, and elemental carbon at the Fresno Supersite, California, *Atmos. Res.*, 93, 874–887, 2009.
- Conny, J. M., Klinedinst, D. B., Wight, S. A., and Paulsen, J. L.: Optimizing thermal-optical methods for measuring atmospheric elemental (black) carbon: a response surface study, *Aerosol Sci. Technol.*, 37, 703–723, 2003.
- Ding, Y. M., Pang, Y. B., and Eatough, D. J.: High-volume diffusion denuder sampler for the routine monitoring of fine particulate matter: I. design and optimization of the PC-BOSS, *Aerosol Sci. Technol.*, 36, 369–382, 2002.
- Ding, A. J., Wang, T., Thouret, V., Cammas, J.-P., and Nédélec, P.: Tropospheric ozone climatology over Beijing: analysis of aircraft data from the MOZAIK program, *Atmos. Chem. Phys.*, 8, 1–13, doi:10.5194/acp-8-1-2008, 2008.
- Eatough, D. J., Wadsworth, A., Eatough, D. A., Crawford, J. W., Hansen, L. D., and Lewis, E. A.: A multiple-system, multi-channel diffusion denuder sampler for the determination of fine-particulate organic material in the atmosphere, *Atmos. Environ.*, 27A, 1213–1219, 1993.
- Eatough, D. J., Obeidi, F., Pang, Y. B., Ding, Y. M., Eatough, N. L., and Wilson, W. E.: Integrated and real-time diffusion denuder sampler for PM_{2.5}, *Atmos. Environ.*, 33, 2835–2844, 1999.
- Eatough, D. J., Eatough, N. L., Obeidi, F., Pang, Y. B., Modey, W., and Long, R.: Continuous determination of PM_{2.5} mass, including semi-volatile species, *Aerosol Sci. Technol.*, 34, 1–8, 2001.
- Eatough, D. J., Eatough, N. L., Pang, Y., Sizemore, S., Kirchstetter, T. W., Novakov, T., and Hobbs, P. V.: Semivolatile particulate organic material in southern Africa during SAFARI 2000, *J. Geophys. Res.*, 108(D13), 8479, doi:10.1029/2002JD002296, 2003.
- Fan, X. H., Brook, J., and Mabury, S. A.: Sampling atmospheric carbonaceous aerosols using an integrated organic gas and particulate sampler, *Environ. Sci. Technol.*, 37, 3145–3151, 2003.
- Fan, X. H., Brook, J. R., and Mabury, S. A.: Measurement of organic and elemental carbon associated with PM_{2.5} during Pacific 2001 study using an integrated organic gas and particle sampler, *Atmos. Environ.*, 38, 5801–5810, 2004.
- Fitz, D. R.: Reduction of the positive organic artifact on quartz filters, *Aerosol Sci. Technol.*, 12, 142–148, 1990.
- Goldfarb, J. L. and Suuberg, E. M.: Vapor pressures and thermodynamics of oxygen-containing polycyclic aromatic hydrocarbons measured using Knudsen effusion, *Environ. Toxicol. Chem.*, 27, 1244–1249, 2008.
- Grover, B. D., Kleinman, M., Eatough, N. L., Eatough, D. J., Cary, R. A., Hopke, P. K., and Wilson, W. E.: Measurement of fine particulate matter nonvolatile and semi-volatile organic material with the Sunset laboratory carbon aerosol monitor, *J. Air Waste Manage. Assoc.*, 58, 72–77, 2008a.
- Grover, B. D., Eatough, N. L., Woolwine, W. R., Cannon, J. P., Eatough, D. J., and Long, R. W.: Semi-continuous mass closure of the major components of fine particulate matter in Riverside, CA, *Atmos. Environ.*, 42, 250–260, 2008b.
- Gundel, L. A., Lee, V. C., Mahanama, K. R. R., Stevens, R. K., and

- Daisey, J. M.: Direct determination of the phase distributions of semi-volatile polycyclic aromatic hydrocarbons using annular denuders, *Atmos. Environ.*, 29, 1719–1733, 1995.
- Hand, J. L., Malm, W. C., Laskin, A., Day, D., Lee, T., Wang, C., Carrico, C., Carrillo, J., Cowin, J. P., Collett, J., and Iedema, M. J.: Optical, physical, and chemical properties of tar balls observed during the Yosemite Aerosol Characterization Study, *J. Geophys. Res.*, 110, D21210, doi:10.1029/2004JD005728, 2005.
- Hering, S. V., Appel, B. R., Cheng, W., Salaymeh, F., Cadle, S. H., Mulawa, P. A., Cahill, T. A., Eldred, R. A., Surovik, M., Fitz, D., Howes, J. E., Knapp, K. T., Stockburger, L., Turpin, B. J., Huntzicker, J. J., Zhang, X. Q., and McMurry, P. H.: Comparison of sampling methods for carbonaceous aerosols in ambient air, *Aerosol Sci. Technol.*, 12, 200–213, 1990.
- Heintzenberg, J.: Size-segregated measurements of particulate elemental carbon and aerosol light absorption at remote Arctic locations, *Atmos. Environ.*, 16, 2461–2469, 1982.
- Hitzenberger, R., Petzold, A., Bauer, H., Ctyroky, P., Pouresmael, P., Laskus, L., and Puxbaum, H.: Intercomparison of thermal and optical measurement methods for elemental carbon and black carbon at an urban location, *Environ. Sci. Technol.*, 40, 6377–6383, 2006.
- Huntzicker, J. J., Johnson, R. L., Shah, J. J., and Cary, R. A.: Analysis of organic and elemental carbon in ambient aerosols by a thermal-optical method. Particulate carbon: atmospheric life cycle, edited by: Wolff, G. T. and Klimisch, R. L., Plenum Press, New York, 79–85, 1982.
- Kirchstetter, T. W., Corrigan, C. E., and Novakov, T.: Laboratory and field investigation of the adsorption of gaseous organic compounds onto quartz filters, *Atmos. Environ.*, 35, 1663–1671, 2001.
- Kirchstetter, T. W. and Novakov, T.: Evidence that the spectral dependence of light absorption by aerosols is affected by organic carbon, *J. Geophys. Res.*, 109, D21208, doi:10.1029/2004JD004999, 2004.
- Lane, D. A., Peters, A. J., Gundel, L. A., Jones, K. C., and Northcott, G. L.: Gas/particle partition measurement of PAH at the Hazelrigg, UK, *Polycycl. Aromat. Compd.*, 20, 225–234, 2000.
- Lewtas, J. L., Pang, Y. B., Booth, D., Reimer, S., Eatough, D. J., and Gundel, L. A.: Comparison of sampling methods for semi-volatile organic carbon associated with PM_{2.5}, *Aerosol Sci. Technol.*, 34, 9–22, 2001.
- Lin, W. L., Xu, X. B., Ge, B. Z., and Zhang, X. C.: Characteristics of gaseous pollutants at Gucheng, a rural site southwest of Beijing, *J. Geophys. Res.*, 114, D00G14, doi:10.1029/2008JD010339, 2009.
- Liu, Y., Sklorz, M., Schnelle-Kreis, J., Orasche, J., Ferge, T., Kettrup, A., and Zimmermann, R.: Oxidant denuder sampling for analysis of polycyclic aromatic hydrocarbons and their oxygenated derivatives in ambient aerosol: evaluation of sampling artifact, *Chemosphere*, 62, 1889–1898, 2006.
- Lukács, H., Gelencsér, A., Hammer, S., Puxbaum, H., Pio, C., Legrand, M., Kasper-Giebl, A., Handler, M., Limbeck, A., Simpson, D., and Preunkert, S.: Seasonal trends and possible sources of brown carbon based on 2-year aerosol measurements at six sites in Europe, *J. Geophys. Res.*, 112, doi:10.1029/2006JD008151, D23S18, 2007.
- Mader, B. T., Flagan, R. C., and Seinfeld, J. H.: Sampling atmospheric carbonaceous aerosols using a particle trap impactor/denuder sampler, *Environ. Sci. Technol.*, 35, 4857–4867, 2001.
- McDow, S. R. and Huntzicker, J. J.: Vapor adsorption artifact in the sampling of organic aerosol: face velocity effects, *Atmos. Environ.*, 24A, 2563–2571, 1990.
- McMurry, P. H. and Zhang, X.: Size distributions of ambient organic and elemental carbon, *Aerosol Sci. Technol.*, 10, 430–437, 1989.
- Menichini, E.: On-filter degradation of particle-bound benzo[a]pyrene by ozone during air sampling: a review of the experimental evidence of an artifact, *Chemosphere*, 77, 1275–1284, 2009.
- Modey, W. K., Pang, Y. B., Eatough, N. L., and Eatough, D. J.: Fine particulate (PM_{2.5}) composition in Atlanta, USA: assessment of the particle concentrator-Brigham Young University organic sampling system, PC-BOSS, during the EPA Supersite study, *Atmos. Environ.*, 35, 6493–6502, 2001.
- Olson, D. A. and Norris, G. A.: Sampling artifacts in measurement of elemental and organic carbon: low-volume sampling in indoor and outdoor environments, *Atmos. Environ.*, 39, 5437–5445, 2005.
- Pang, Y. B., Gundel, L. A., Larson, T., Finn, D., Liu, L. J. S., and Claiborn, C. S.: Development and evaluation of a personal particulate organic and mass sampler, *Environ. Sci. Technol.*, 36, 5205–5210, 2002.
- Pósfai, M., Gelencsér, A., Simonics, R., Arató, K., Li, J., Hobbs, P. V., and Buseck, P. R.: Atmospheric tar balls: particles from biomass and biofuel burning, *J. Geophys. Res.*, 109, D06213, doi:10.1029/2003JD004169, 2004.
- Possanzini, M., Di Palo, V., Tagliacozzo, G., and Cecinato, A.: Physico-chemical artefacts in atmospheric PAH denuder sampling, *Polycycl. Aromat. Compd.*, 26, 185–195, 2006.
- Reisinger, P., Wonaschütz, A., Hitzenberger, R., Petzold, A., Bauer, H., Jankowski, N., Puxbaum, H., Chi, X., and Maenhaut, W.: Intercomparison of measurement techniques for black or elemental carbon under urban background conditions in wintertime: influence of biomass combustion, *Environ. Sci. Technol.*, 42, 884–889, 2008.
- Schauer, J. J., Mader, B. T., DeMinter, J. T., Heidemann, G., Bae, M. S., Seinfeld, J. H., Flagan, R. C., Cary, R. A., Smith, D., Huebert, B. J., Bertram, T., Howell, S., Kline, J. T., Quinn, P., Bates, T., Turpin, B., Lim, H. J., Yu, J. Z., Yang, H., and Keywood, M. D.: ACE-Asia intercomparison of a thermal-optical method for the determination of particle-phase organic and elemental carbon, *Environ. Sci. Technol.*, 37, 993–1001, 2003a.
- Schauer, C., Niessner, R., and Pöschl, U.: Polycyclic aromatic hydrocarbons in urban air particulate matter: decadal and seasonal trends, chemical degradation, and sampling artifacts, *Environ. Sci. Technol.*, 37, 2861–2868, 2003b.
- Sciare, J., Cachier, H., Oikonomou, K., Ausset, P., Sarda-Estève, R., and Mihalopoulos, N.: Characterization of carbonaceous aerosols during the MINOS campaign in Crete, July–August 2001: a multi-analytical approach, *Atmos. Chem. Phys.*, 3, 1743–1757, doi:10.5194/acp-3-1743-2003, 2003.
- Sciare, J., Oikonomou, K., Favez, O., Liakakou, E., Markaki, Z., Cachier, H., and Mihalopoulos, N.: Long-term measurements of carbonaceous aerosols in the Eastern Mediterranean: evidence of long-range transport of biomass burning, *Atmos. Chem. Phys.*, 8, 5551–5563, doi:10.5194/acp-8-5551-2008, 2008.

- Solomon, P., Baumann, K., Edgerton, E., Tanner, R., Eatough, D., Modey, W., Maring, H., Savoie, D., Natarajan, S., Meyer, M. B., and Norris, G.: Comparison of integrated samplers for mass and composition during the 1999 Atlanta Supersites project, *J. Geophys. Res.*, 108(D7), 8423, doi:10.1029/2001JD001218, 2003.
- Strommen, M. R. and Kamens, R. M.: Simulation of semivolatile organic compound microtransport at different times scales in airborne diesel soot particles, *Environ. Sci. Technol.*, 33, 1738–1746, 1999.
- Subramanian, R., Khlystov, A. Y., Cabada, J. C., and Robinson, A. L.: Positive and negative artifacts in particulate organic carbon measurement with denuded and undenuded sampler configurations, *Aerosol Sci. Technol.*, 38, 27–48, 2004.
- Subramanian, R., Khlystov, A. Y., and Robinson, A. L.: Effect of peak inert-mode temperature on elemental carbon measured using thermal-optical analysis, *Aerosol Sci. Technol.*, 40, 763–780, 2006.
- Swartz, E., Stockburger, L., and Vallero, D. A.: Polycyclic aromatic hydrocarbons and other semivolatile organic compounds collected in New York city in response to the events of 9/11, *Environ. Sci. Technol.*, 37, 3537–3546, 2003.
- Tang, H., Lewis, E. A., Eatough, D. J., Burton, R. M., and Farber, R. J.: Determination of the particle size distribution and chemical composition of semi-volatile organic compounds in atmospheric fine particles, *Atmos. Environ.*, 28, 939–947, 1994.
- Tang, G., Li, X., Wang, Y., Xin, J., and Ren, X.: Surface ozone trend details and interpretations in Beijing, 2001–2006, *Atmos. Chem. Phys.*, 9, 8813–8823, doi:10.5194/acp-9-8813-2009, 2009.
- Tsapakis, M. and Stephanou, E. G.: Collection of gas and particle semi-volatile organic compounds: use of an oxidant denuder to minimize polycyclic aromatic hydrocarbons degradation during high-volume air sampling, *Atmos. Environ.*, 37, 4935–4944, 2003.
- Turpin, B. J. and Lim, H. J.: Species contributions to PM_{2.5} mass concentrations: revisiting common assumptions for estimating organic mass, *Aerosol Sci. Technol.*, 35, 602–610, 2001.
- van Poppel, L. H., Friedrich, H., Spinsby, J., Chung, S. H., Seinfeld, J. H., and Buseck, P. R.: Electron tomography of nanoparticle clusters: implications for atmospheric lifetimes and radiative forcing of soot, *Geophys. Res. Lett.*, 32, L24811, doi:10.1029/2005GL024461, 2005.
- Viana, M., Chi, X., Maenhaut, W., Cafmeyer, J., Querol, X., Alastuey, A., Mikuška, P., and Večeřa, Z.: Influence of sampling artefacts on measured PM, OC, and EC levels in carbonaceous aerosols in an urban area, *Aerosol Sci. Technol.*, 40, 107–117, 2006a.
- Viana, M., Chi, X., Maenhaut, W., Querol, X., Alastuey, A., Mikuška, P., and Večeřa, Z.: Organic and elemental carbon concentrations in carbonaceous aerosols during summer and winter sampling campaigns in Barcelona, Spain, *Atmos. Environ.*, 40, 2180–2193, 2006b.
- Wang, S. X., Zhao, M., Xing, J., Wu, Y., Zhou, Y., Lei, Y., He, K. B., Fu, L. X., and Hao, J. M.: Quantifying the air pollutants emission reduction during the 2008 Olympic Games in Beijing, *Environ. Sci. Technol.*, 44, 2490–2496, 2010.
- Watson, J. G., Chow J. C., and Chen L. A.: Summary of organic and elemental carbon/black carbon analysis methods and inter-comparisons, *Aerosol Air Qual. Res.*, 5, 65–102, 2005.
- Wonaschütz, A., Hitzemberger, R., Bauer, H., Pournesmaeil, P., Klatzer, B., Caseiro, A., and Puxbaum, H.: Application of the integrating sphere method to separate the contributions of brown and black carbon in atmospheric aerosols, *Environ. Sci. Technol.*, 43, 1141–1146, 2009.
- Yang, H. and Yu, J. Z.: Uncertainties in charring correction in the analysis of elemental and organic carbon in atmospheric particles by thermal/optical methods, *Environ. Sci. Technol.*, 36, 5199–5204, 2002.
- Yu, J. Z., Xu, J. H., and Yang, H.: Charring characteristics of atmospheric organic particulate matter in thermal analysis, *Environ. Sci. Technol.*, 36, 754–761, 2002.
- Zheng, M., Cass, G. R., Schauer, J. J., and Edgerton, E. S.: Source apportionment of PM_{2.5} in the southeastern United States using solvent-extractable organic compounds as tracers, *Environ. Sci. Technol.*, 36, 2361–2371, 2002.